Time reconstructions in light-in-flight recording by holography

Nils Abramson

When light-in-flight recording by holography is used two different sorts of apparent distortion of the wavefronts exist. The first distortion is common to all types of ultrafast gating viewing system and like relativistic phenomena it is caused by the limited speed of light used for observation. The second distortion is produced by the holographic process itself and is caused by the limited speed of the light pulse used as a reference beam. By using the second distortion to compensate for the first it is possible to manipulate or eliminate apparent wavefront tilts or distortions so that measurement of the 3-D shape of wavefronts or other objects is facilitated. A reconstruction beam that is the conjugate of the reference beam results in three interesting effects, one of which is the reemission of the recorded pulse.

I. Introduction

A point source of light (A) produced an ultrashort (picosecond) pulse that expands like a spherical shell of light. If the space around A is filled with scattering particles and also larger objects, the position, shape, and velocity of this shell can be observed where it intersects the scattering surfaces. To make such an observation, however, an ultrafast (picosecond) shutter is needed.

A picosecond light pulse used as the reference beam in a holographic recording works like an ultrafast light shutter which makes it possible to produce a frameless, continuous, moving picture of the spherical wavefront, or rather pulse front, as it moves with the speed of light.[1-3] Let the position of the point of observation (B) be identical to that of the point of illumination (A). Light has to move out to the scattering particles and back again before it can be observed. During the time light is traveling back the unscattered wavefront is moving further out so that, when the observation is made, the true wavefront has traveled out to twice the observed radius. Thus the radius of the spherical light shell appears to be half of its true value at the time of observation. This is also the case for the thickness and velocity of the light shell.

If there is a separation between A and B, the spheres appear to be transformed into ellipsoids. The reason is that only those particles appear illuminated for which the time of flight for light from A to B via the particles (C) is equal to the delay between emission of the pulse at A and the observation at B. If the speed of light is constant within the studied volume, constant time of flight is equal to constant path length. An ellipsoid represents constant path length of light emitted from one focal point (A) and reflected by the surface of the ellipsoid to the other focal point (B).

These ellipsoids of constant path length have already been used in holography to optimize the use of a short coherent length and to evaluate interference fringes.[4] It has been named the holodiagram (Fig. 1) and is based on a set of ellipses, each of which represents a constant path length of light emitted from one focal point (A) scattered by an object (C) on the surface of the ellipsoid toward the observation at the other focal point (B). Adjacent ellipses represent a constant path length difference. The k-value (Fig. 2) is a measure of the separation of the ellipses which varies between half of the path length difference at the x-axis outside A–B to an infinite value between A and B. It has a constant value along arcs of circles through A and B, because the k-value is a function ($1/\cos\alpha$) of angle ACB (2α).

Thus we have demonstrated that, when A and B are separated, the true spherical shells appear to be transformed into the ellipsoids of the holodiagram. Adjacent ellipsoids represent a constant path length difference and thus their separation represents the apparent separation of the spheres and the velocity of the ellipsoids represent the apparent speed of the spheres.

The author is with Royal Institute of Technology, Industrial Metrology Department, S-100 44 Stockholm 70, Sweden.

Received 13 November 1989.
0003-6935/91/101242-11$05.00/0.

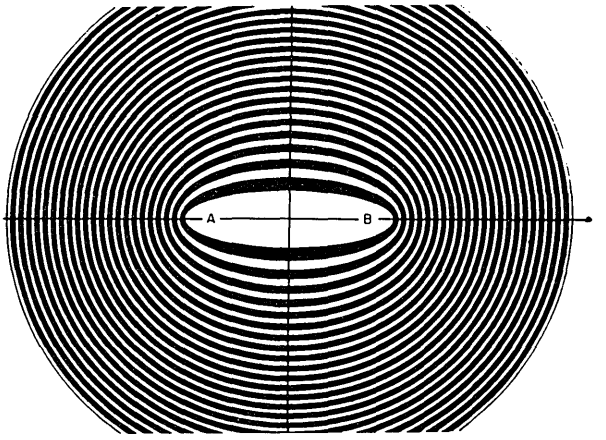

Fig. 1. Holodiagram consisting of a set of concentric ellipses representing constant path length for light from A to B. Adjacent ellipses represent a constant difference in path length, which could represent wavelength, coherence length, or pulse length.

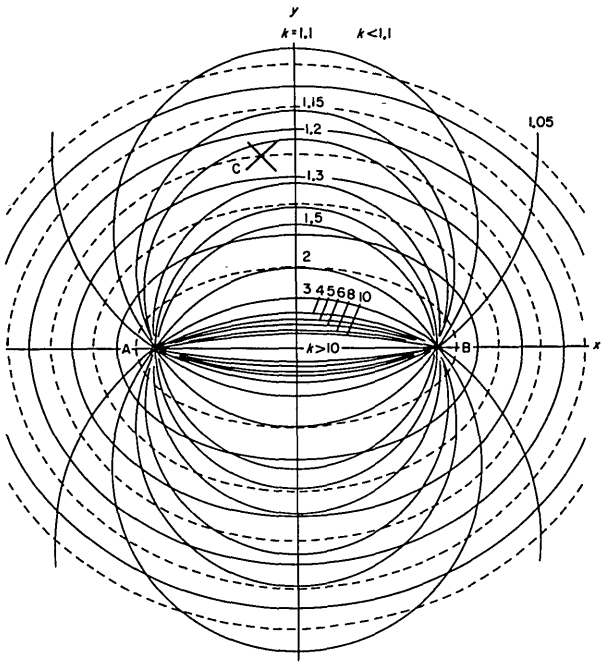

Fig. 2. Separation of the ellipses of the holodiagram varies by a factor k which is constant along arcs of circles through A and B. Thus the apparent values of wavelength, coherence length, and pulse length are found by multiplying the true values by k.

Thus we can say that the apparent pulse length and the apparent velocity of light are both 0.5 k times their true value.

II. Distortions Caused by a Hologram Plate

Thus, when any sort of gated viewing system is used the spherical wavefronts appear transformed into ellipsoids if there is a separation between the light source and the observer. When light-in-flight recording by holography is used another type of distortion also exists which is caused by the angle of the reference beam in combination with the distance of the point of observation from the hologram plate.[5] When the observing eye or camera lens is close to the plate, the ellipsoids are observed undistorted. If, however, the observation is made further away from the plate, different angles of view represent different points of time, because different parts of the hologram plate are used for reconstruction and these different parts were recorded during different points of time.

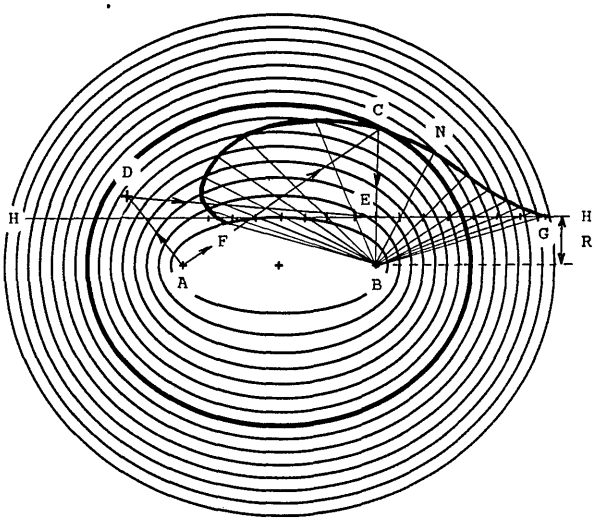

Fig. 3. Ellipses studied from point B at a distance R behind hologram plate H, which is illuminated by the reference beam from D. In that case the ellipses appear distorted, e.g., from the ellipse of the holodiagram that passes through C to curve FCG. This distortion is caused by the time it takes for the pulse from D to travel along the hologram plate.

Let, for example, the reference pulse illuminate the plate from the left during exposure of the hologram. Then this reference pulse works like a curtain shutter that, with a speed close to that of light, moves from left to right, first making the left part and last the right part of the plate sensitive to holographic recording.

When we later reconstruct the processed plate and look through the left part of the hologram plate we see what happened first to the recorded object. If we look through a part of the plate that is further to the right we see what happened later to the object. The total time span recorded by the plate is the time it took the reference pulse to pass along the whole plate from left to right. As the ellipsoids expand (with a speed that might exceed c) their left part appears contracted while their right part appears expanded.

The situation described is demonstrated in Fig. 3 where A is the light source (e.g., the pinhole in a spatial filter), B is the point of observation (e.g., a small aperture of a camera), C is a studied object point, and D is the point source of the reference beam. H–H is the hologram plate, while R is the distance behind the plate from which the observation is made.

When R is zero, the whole object is observed through one point on the hologram plate which represents one point of time, and therefore the spheres around A appear to be ellipsoids with A and B as focal points. When R is nonzero, the left part of the ellipsoids will be

seen through a part on the plate that during exposure was closer to the reference beam (D) and thus was exposed earlier when the ellipsoid was smaller. Consequently the right part of the ellipsoid will appear larger.

In the diagram of Fig. 3 each point on the surface of the hologram plate has been marked out where the path length from D has changed by the same constant amount as the path length difference separating adjacent ellipsoids. Straight lines of sight from B have been drawn combining points on the plate with points on the ellipsoids having identical path lengths. (Object beam path length ACE is equal to reference beam path length ADE.)

Thus we find from Fig. 3 that the curve (FCG) produced in this way differs substantially from the ellipse of the holodiagram that passes through C. It is possible that this effect could be of advantage in either of the following uses:

(1) To transform the apparent ellipsoidal wavefronts back into the original spherical wavefronts. This result would simplify the study of the shape of the true wavefront.

(2) To tilt the interesting apparent wavefront until it is perpendicular to the line of sight (e.g., BN). This result would simplify the measurement of an object's 3-D shape by studying its intersections with the wavefronts.

(3) To straighten the curvature of the ellipsoids so that a flatter surface is formed (e.g., CG). Again the result would simplify 3-D measurements by reducing or eliminating the need for collimated illumination and observation.

III. Calculations

To get a closer view of these possibilities we now study the shape of the curve (FCG) in a general mathematical way. From Fig. 4 we derive the following equations:

$$\frac{x^2}{a^2}+\frac{y^2}{b^2}=1, \tag{1}$$

$$L=a, \tag{2}$$

$$L^2=c^2+b^2, \tag{3}$$

where ($2L$) represents the constant path length of light emitted by A and observed from B. Combining Eqs. (1), (2), and (3) produces

$$\frac{x^2}{L^2}+\frac{y^2}{L^2-C^2}=1, \tag{4}$$

where L is not a constant but a function of x and y as found from Fig. 3:

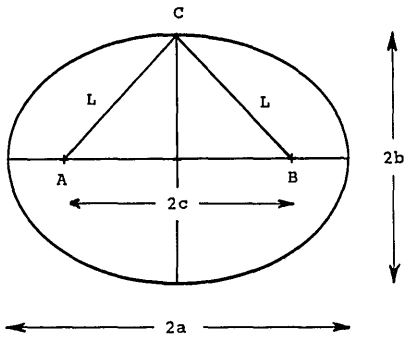

Fig. 4. Equation of an ellipse is usually expressed in a and b. To express the path lengths of Fig. 3 we prefer to use distances L and c.

$$2L=AD+DE+EB. \tag{5}$$

Let us change the origin of coordinates to B:

$$2L=AD+\sqrt{(y_D-y_H)^2+(x_D-x_H)^2}+\sqrt{x_H^2+y_H^2}. \tag{6}$$

Equation (4) is transformed into

$$\frac{(x-c)^2}{L^2}+\frac{y^2}{L^2-C^2}=1, \tag{7}$$

$$x_H=x\frac{y_H}{y}. \tag{8}$$

Combining Eqs. (6), (7), and (8) results in

$$\frac{(x-c)^2}{\left\{0{,}5\left[AD+\sqrt{(y_D-y_H)^2+\left(x\frac{y_H}{y}-x_D\right)^2}\right]+y_H\sqrt{\frac{x^2}{y^2}+1}\right\}^2}+\frac{y^2}{\left\{0{,}5\left[AD+\sqrt{(y_D-y_H)^2+\left(x\frac{y_H}{y}-x_D\right)^2}\right]+y_H\sqrt{\frac{x^2}{y^2}+1}\right\}^2-C^2}=1. \tag{9}$$

Let us check Eq. (9) for $y_H=R=0$:

$$\frac{(x-c)^2}{[0{,}5(AD+\sqrt{y_D^2+x_D^2})]^2}+\frac{y^2}{[0{,}5(AD+\sqrt{y_D^2+x_D^2})]^2-C^2}=1. \tag{10}$$

This result is correct because it is the equation of one of the ellipses of the holodiagram.

If the reference beam is parallel to the hologram plate, y_D will be equal to y_H and Eq. (8) will be simplified to

$$\frac{(x-c)^2}{\left[0{,}5\left(AD+x\frac{y_H}{y}-x_D\right)+y_H\sqrt{\frac{x^2}{y^2}+1}\right]^2}+\frac{y^2}{\left[0{,}5\left(AD+\frac{y_H}{y}-x_D\right)+y_H\sqrt{\frac{x^2}{y^2}+1}\right]^2-C^2}=1. \tag{11}$$

IV. Compensations

Let us now study some practical special cases for which we do not have to use the complicated general Eq. (9). First we determine how to plan the setup to contour 3-D objects. Object C is intersected by a thin sheet of light (Fig. 5). If illumination A and observa-

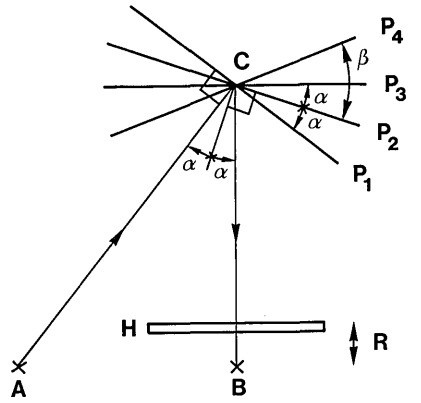

Fig. 5. Light source A illuminates a smoke-filled box at C and the pulse front is observed from B behind hologram plate H. Angle ACB is 2α. The true pulse front (P_1) is perpendicular to AC, but because of the limited speed of light it appears to be rotated by angle α so that it becomes normal to the bisector of ACB (P_2). Because of the holographic process it appears further rotated by angle β to P_4. By observing the reconstruction of C from a certain distance R behind H, angle β can be given such a value that the pulse front (P_3) appears perpendicular to the line of observation (C–B), which is often advantageous for measuring purposes.

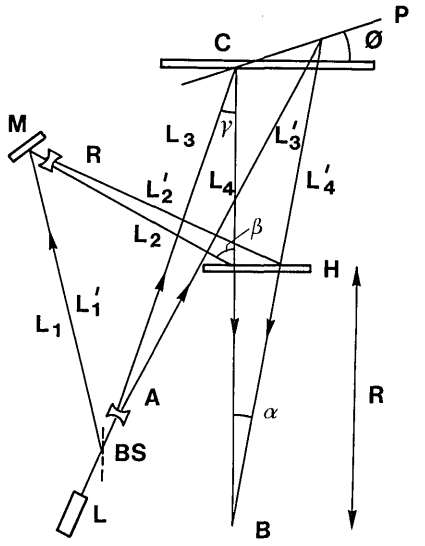

Fig. 6. Light from laser L illuminates by diverging lens A the object at C and hologram plate H is illuminated by diverging lens R via mirror M. The object is observed from B which is at a distance R behind the plate. A necessary condition for holographic recording with an ultrashort pulse from A is that $L_1 + L_2 = L_3 + L_4$.

tion B are made from two points close together and far from a small object, the intersecting sheet can be approximated into a flat surface perpendicular both to the line of illumination AC and to the line of sight CB. When the separation between A and B is made larger, the true intersecting plane is tilted by angle 2α in relation to the normal of the line of sight where 2α is angle ACB. To the observer, however, it appears to be tilted only half that much by angle α. If finally a hologram with an oblique reference pulse is used for registration, the intersecting plane can be tilted by still another angle (e.g., β in Fig. 5), the magnitude of which depends on the separation (R) of the point of observation from the hologram plane.

Thus by varying α and R it is possible to make the intersection at a preferred angle. Usually it is advantageous to have the plane perpendicular to the line of sight, so let us study this case when β is equal to α but of opposite sign.

Let us study Fig. 6, where A is the point of illumination (spatial filter), B is the point of observation at distance R behind hologram plate H, M is a mirror for the reference beam, and C is the object the 3-D shape of which is to be measured by sectioning with thin light sheet P, which is tilted at angle ϕ in relation to the normal to the line of sight. Light source L is a laser producing ultrashort pulses.

For holographic recording it is necessary that the path lengths from laser to holgram plate are the same for the reference and object beams. Thus

$$L_1 + L_2 = L_3 + L_4. \tag{12}$$

Now we study the changes in path lengths that are caused if the line of sight B–C is slightly changed by angle α. Even after this change Eq. (12) should still be satisfied. Thus

$$L_1' + L_2' = L_3' + L_4', \tag{13}$$

$$L_1' = L_1 \text{ because } L_1 \text{ is independent of } \alpha, \tag{14}$$

$$(L_2')^2 = (R\tan\alpha)^2 + L_2^2 - 2L_2R\tan\alpha\cos(\beta + 90), \tag{15}$$

$$(L_3')^2 = L_3^2 + S^2 - 2L_3S\cos(\gamma + 90 + \phi), \tag{16}$$

$$S = \frac{(L_4 + R)\sin\alpha}{\cos(\alpha + \phi)}, \tag{17}$$

$$L_4' = \frac{(L_4 + R)\sin(90 + \phi)}{\sin(\alpha + 90 + \phi)} - \frac{R}{\cos\alpha}. \tag{18}$$

Approximations for small angle α are

$$L_2' = R\tan\alpha\sin\beta + L_2, \tag{19}$$

$$L_3' = \frac{(L_4 + R)\sin\alpha}{\cos\phi}\sin(\gamma + \phi) + L_3, \tag{20}$$

$$L_4' = (L_4 + R)\tan\alpha\tan\phi + L_4. \tag{21}$$

Inserting Eqs. (14), (19), (20), and (21) into Eq. (13) results in a general equation from which angle ϕ of the apparent pulse front can be calculated:

$$\tan\phi = \frac{1}{1 + \cos\gamma}\left(\frac{R\sin\beta}{L_4 + R} - \sin\gamma\right). \tag{22}$$

It is interesting to find that, for the setup in Fig. 6, there are only two ways to reach the maximum value of $\phi = 90°$. Either $\gamma = 180°$, which represents objects studied in transmission, or $L_4 = -R_1$, which represents an object image between observer and hologram plate. The latter condition is reached simply by studying the pseudoscopic image instead of the ordinary virtual image seen in Fig. 6. Both situations are described in later sections of this paper.

Let us test Eq. (22) by inserting $R = 0$ and $\gamma = 90°$. The equation correctly results in a relativistic rotation

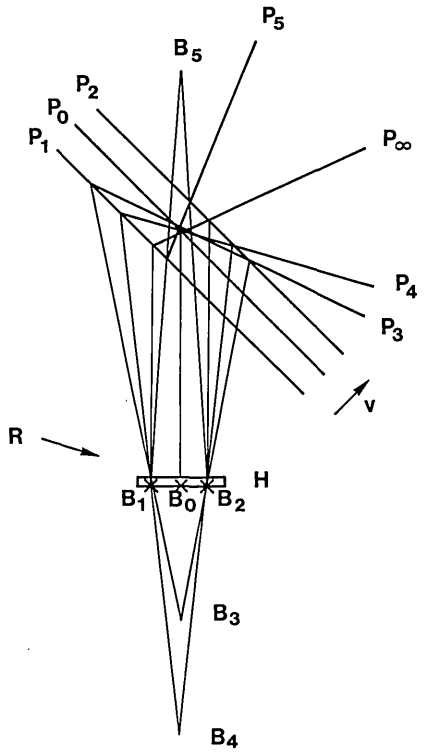

Fig. 7. Hologram plate H reconstructs pulse front P by use of reference pulse R. The reconstructed pulse front, which moves with apparent speed v, appears to be at P_0, P_1, and P_2 when studied from B_0, B_1, and B_2, respectively. When studied from B_3 it appears to be at P_3 and from B_4 at P_4. If we move B_0 to an infinite distance the apparent pulse front is P_∞. If we study the pseudoscopic image from B_5 the pulse front appears to be at P_5.

of the apparent wavefront of 45° which is independent of β and thus of the holographic process.

Is it possible to find such conditions in which there is no angle separating the apparent pulse front from the true pulse front? To test this possibility insert $\phi = -\gamma$ into Eq. (22). The result is

$$\tan\gamma = -\frac{R\sin\beta}{2(L_4 + R)}). \tag{23}$$

Thus the apparent and true wavefronts are identical if γ is zero and either R or β or both are zero. This result is correct and agrees with experiments.

Are there other not quite as trivial solutions? Let us, e.g., insert $\gamma = 10°$ and $R = L_4$ into Eq. (23). The result is $\beta = -45°$.

Thus, if the object, e.g., a glass box filled with smoke, is illuminated from the left at an angle γ of 20° and the holographic plate is illuminated from the right at an angle of 46°, the apparent pulse front will be identical to the true pulse front when the eye is placed along L_4 at a distance of L_4 behind the hologram plate.

Let us finally use Eq. (22) to study the conditions for $\phi = 0$ which is usually most convenient for contouring (Figs. 8–12) or for the study of optical delays (Figs. 16–22). The result is

$$\sin\gamma = \frac{R}{L_4 + R}\sin\beta. \tag{24}$$

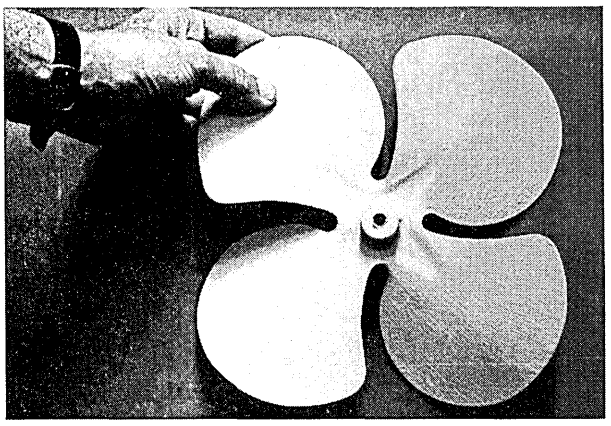

Fig. 8. Three-dimensional shape of this propeller is measured by studying its intersection with a thin sheet of light.

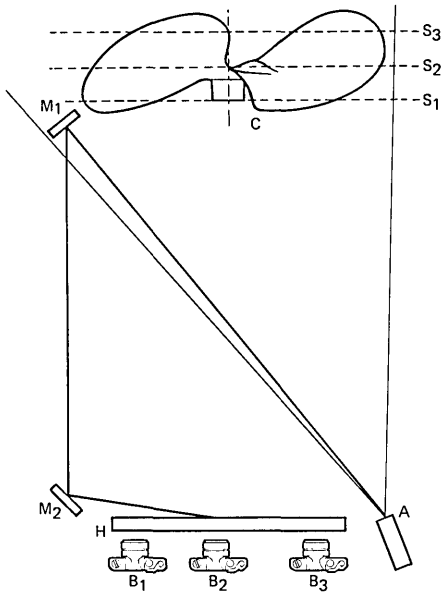

Fig. 9. Picosecond pulse from the laser at A is used both to illuminate the propeller (C) and to produce the reference pulse that illuminates the hologram plate (H) via mirrors M_1 and M_2. From B_1, B_2, and B_3 are, during reconstruction, seen intersections S_1, S_2, and S_3, respectively. The straightness of the intersections is an approximation which could be true only if distance HC were infinite.

Let us study an example. If L_4 is, e.g., 95 cm, β is 30°, and R is 5 cm, then γ is found to be 1.4°. Illumination of the object should be from the same side as the reference beam (left in Fig. 6). Moving the point of observation (the eye or camera) toward the plate results in an apparent clockwise rotation of the intersecting light sheet, while a counterclockwise rotation is produced by moving away from the plate. If moving to an infinite distance does not produce enough rotation, the pseudoscopic image makes it possible to produce still larger rotation as if moving past infinity.

Figure 7 demonstrates how the intersecting light sheet can be found in a simple graphic way. The reference pulse travels along the plate from left to right so that it passes B_1 at time 1 and B_2 at time 2. Similar-

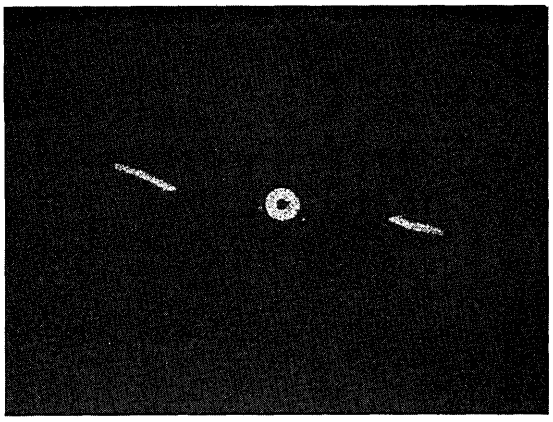

Fig. 10. Photo exposed during reconstruction with the camera positioned at B_1 corresponding to cross section S_1 (Fig. 9). The sheet of light has just reached the hub of the propeller and two of its blades.

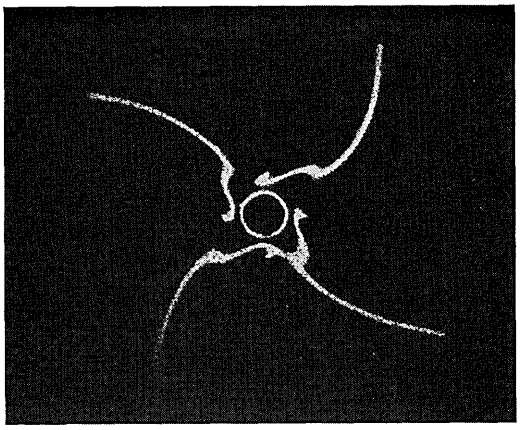

Fig. 11. Camera at B_2 produced cross section S_2. The hub has just passed out of the light into darkness while the four blades and their central joint are intersected.

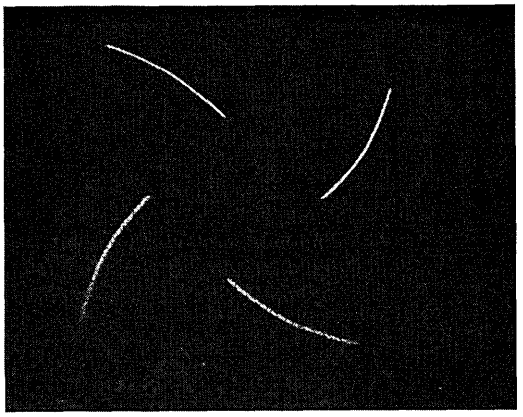

Fig. 12. Light sheet has passed the central joint and the cross sections of the blades reveal their 3-D shape.

ly, the intersecting light sheet passes through the object space passing P_1 at time 1 and P_2 at time 2. Thus P_1 is seen from B_1 and P_2 from B_2.

When the eye during reconstruction is situated at B_0, the corresponding apparent light sheet is P_0. If the

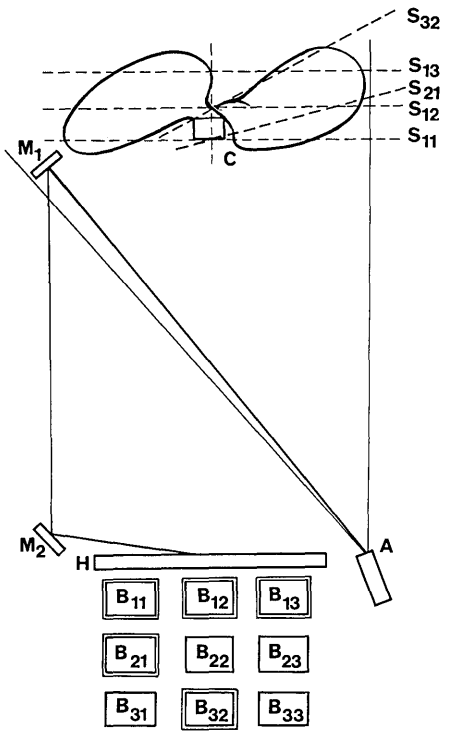

Fig. 13. Same setup as in Fig. 9 but the point of observation (camera) is not only moved along the hologram plate but also backward away from the plate as indicated by squares B_{ik}.

Fig. 14. Same hologram plate as in Figs. 10–12 but studied from a point behind the plate (B_{21}) at about half of the distance the propeller was in front of the plate during the recording. In this case intersecting surface S_{21} is tilted ~20°.

eye is situated at B_3 the corresponding light sheet P_3 is found by connecting the points where B_3B_1 intersects P_1 and B_3B_2 intersects P_2.

Moving the eye further away from the plate to B_4 results in a further counterclockwise rotation of the light sheet to P_4, which is found by connecting the points where B_4B_1 intersects P_1 and B_4B_2 intersects P_2. Moving B to infinity results in P_∞ which is found by drawing vertical lines from B_1 to P_1 and from B_2 to P_2.

If we want to rotate the light sheet still more counterclockwise we must look at the pseudoscopic image,

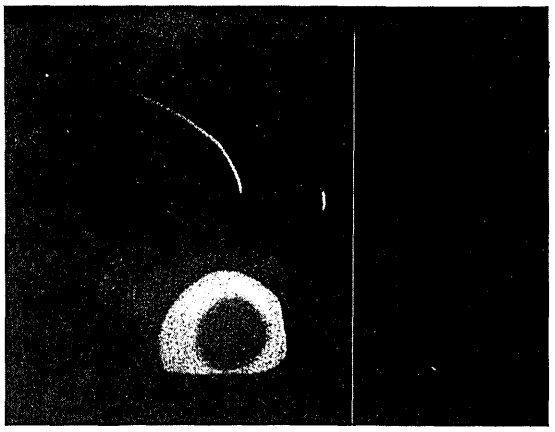

Fig. 15. Same hologram as in Figs. 10–12 but the camera was moved still further away from the plate. The intersecting plate is rotated so that it becomes parallel to a large position of one of the curved blades of the propeller.

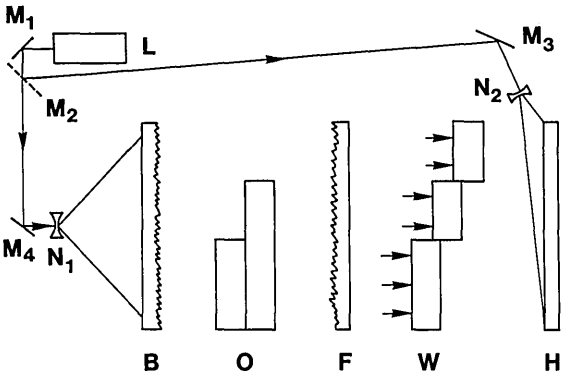

Fig. 16. While the holograms in Figs. 10–15 are all made in reflection, similar methods can be used in transmission. The setup is designed to reveal an object (O) hidden between two scatterplates (B) and (F). The ultrashort laser pulse from L is reflected by mirrors M_1 and M_4, illuminates scatterplate B, and passes through the object (O) resulting in the broken pulse front (W) which reaches the hologram plate (H). The reference pulse is reflected by M_2 and M_3; N_1 and N_2 are two diverging lenses.

e.g., from B_5. The corresponding P_5 is found by connecting the point where B_5B_1 intersects P_1 and B_5B_2 intersects P_3.

V. Practical Examples

As a practical example of the described method to manipulate the intersecting light sheet we study the propeller in Fig. 8. The setup for this contouring experiment is seen in Fig. 9 and the results, by moving the point of observation (camera) along the hologram plate, are presented in Figs. 10, 11, and 12.

When the camera is moved away from the plate ($R \neq 0$) as shown in Fig. 13, the intersecting light sheet is tilted as seen in Fig. 14. Finally, by increasing distance R to ~2 m, the tilt is large enough so that the intersection is parallel to one of the blades (Fig. 15).

Sometimes LIF is used in transmission as a gated viewing system that can penetrate the scattering medium.[6] Such an example is demonstrated in Figs. 16 and 17. By temporal filtering it is possible to study only the light that arrives first after passing the two ground glasses S_1 and S_2. This light travels along the fastest paths which are represented by straight lines, and thus it is the least scattered.

Therefore it can be used to reveal objects positioned between S_1 and S_2 that are totally hidden because their images are drowned by scattered light when they are looked at directly. The object might either be absorbing light or have a speed of light that differs from its surroundings.

For this case we can set up the same equations as for contouring in reflected light. Thus Eqs. (12) and (13) and the resulting Eq. (22) also apply in the transmission configuration of Fig. 17.

It is most convenient when the apparent light sheet is parallel to the observed scatterplate ($\phi = 0$). Thus, as in reflection, we get the equation

$$\sin\gamma = \frac{R}{L_4 + R}\sin\beta. \tag{25}$$

In this case illumination of the object should also be from the same side as the reference beam (left of Fig. 17). Moving the point of observation (the eye or camera) toward the plate, however, results in an apparent counterclockwise rotation of the intersecting light sheet, while a clockwise rotation is produced by moving away from the plate. Even in this case the pseudoscopic view results in still greater clockwise rotation.

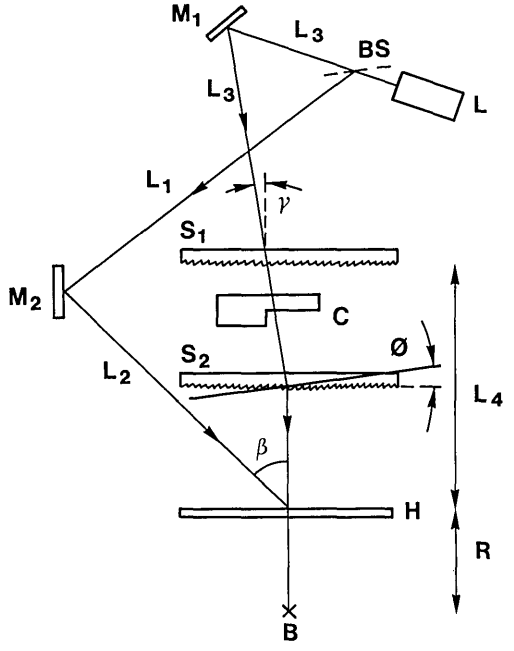

Fig. 17. Light from laser L is divided into object and reference beams by the beam splitter (BS). The object beam is reflected by mirror M_1 and illuminates ground glass screen S_1, passes through the transparent object (C), and reaches the hologram plate (H) after passing through the second ground glass screen S_2. The reference beam is reflected by mirror m_2 toward the hologram plate. A necessary condition for holographic recording with an ultrashort pulse is that $L_1 + L_2 = L_3 + L_4$.

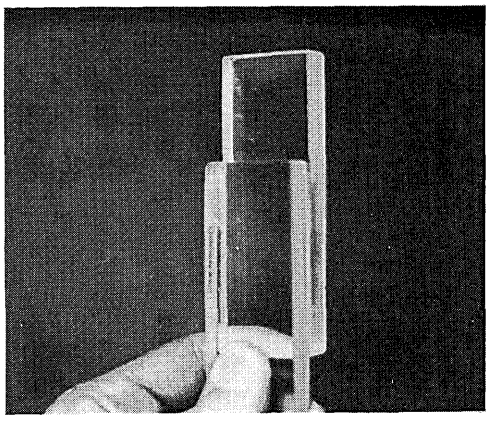

Fig. 18. Transparent object consisting of two pieces of Plexiglas held together so that light at the top had to pass one layer, while light further down had to pass two layers of Plexiglas.

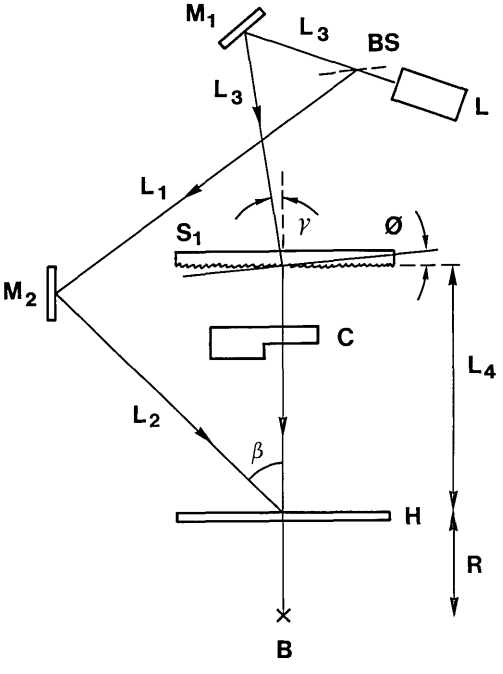

Fig. 19. Setup is similar to that in Fig. 17, but the transparent object (C) is observed directly as it is illuminated by the laser pulse that has passed through ground glass S_1. The angle (ϕ) of the apparent pulse front (P) is a function of the angle of light illuminating S_1, the angle of the reference beam (β), and the relation of R to L_4.

As an example of this method to manipulate the intersecting light sheet we study a slightly different experiment where a Plexiglas object (Fig. 18) is observed, not hidden between two ground glasses, but positioned in front of just one ground glass (S_1), as seen in Fig. 19. Equation (25) still applies but in this case L_3 and L_4 meet at S_1.

When the camera is at a certain distance from the hologram plate the background appears bright, while the light passing through the Plexiglas is delayed so that it is not yet seen (Fig. 20). As the camera is moved to the right we see the object slightly later and the background is now dark because the light pulse has

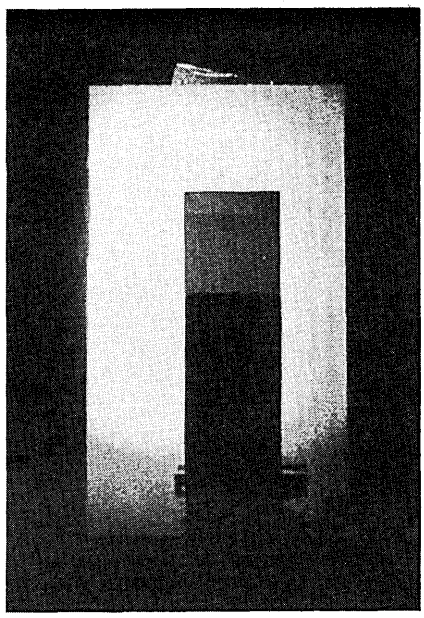

Fig. 20. One single 8-ps pulse is delivered by the laser and the reconstruction is photographed through the left part of the hologram plate with the camera lens at a distance from the plate of ~3 cm. What we see is the first light which arrives all around the Plexiglas.

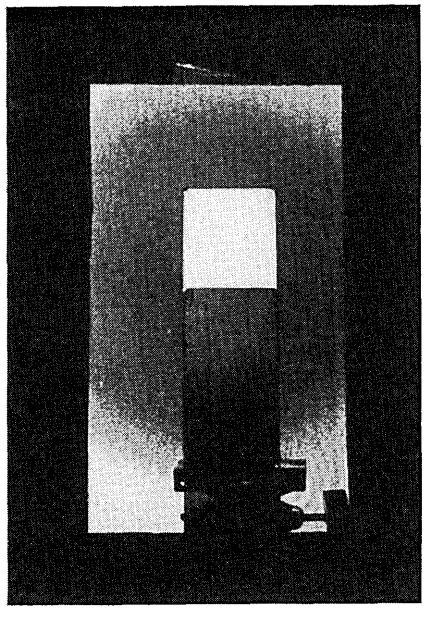

Fig. 21. Photo made through the middle of the plate showing that, after the surrounding light has passed by, the light delayed by one layer of Plexiglas arrives.

passed. The top of the object is however bright because the light delayed by one layer of Plexiglas is now arriving (Fig. 21). Still later the light at the bottom arrived after passing through two layers of Plexiglas (Fig. 22).

Figure 20 shows that, when the camera is at a certain distance R from the hologram plate so that Eq. (24) is satisfied, the whole ground glass appears illuminated simultaneously as if the intersecting light sheet is par-

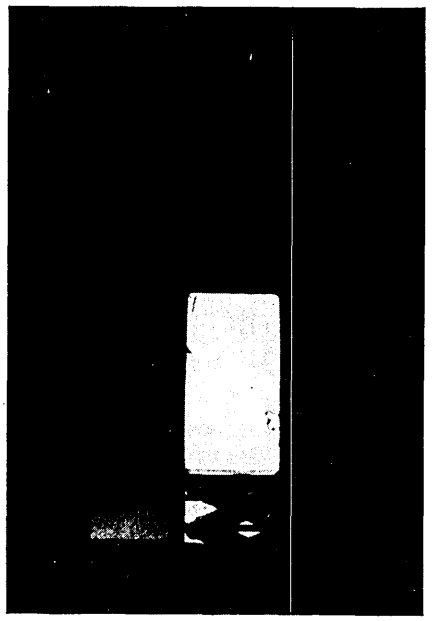

Fig. 22. Photo made through the right part of the plate showing how the light delayed by two layers of Plexiglas arrives.

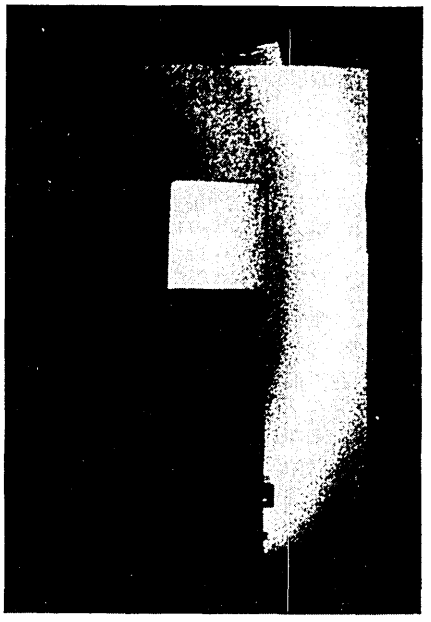

Fig. 23. Photo corresponding to Fig. 21, but the point of observation (the camera lens) is moved further away (0.3 m) from the plate. The result is that the intersecting light sheet appears to be tilted.

allel to the glass surface ($\phi = 0$). This is also the case for Figs. 21 and 22. However, as the camera is moved away from the hologram plate the intersection appears to be tilted clockwise ($\phi > 0$), a bright line moves with time from left to right (Fig. 23). Moving close to the hologram plate results in the line moving in the opposite direction. Finally by studying the pseudoscopic image, the intersection appears still more tilted (Fig. 24).

At the top of Fig. 24 we see the pulse front that

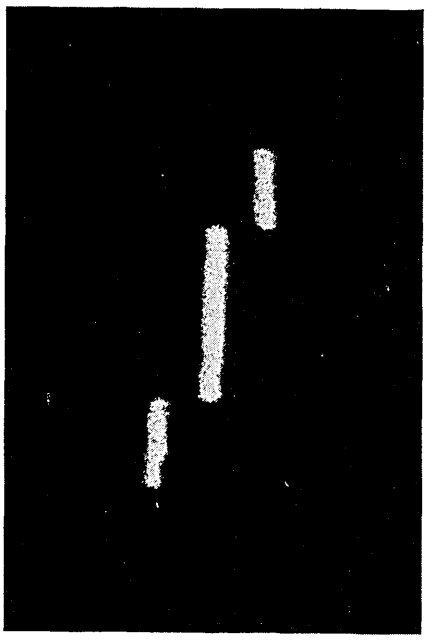

Fig. 24. When looking at the conjugate image of the plate the tilt appears so large that we see the pulse front almost from the side in spite of the fact that it moved straight toward us during recording. The pulse front which is split into three moves from left to right and on the top we see light passing over the Plexiglas. Further down light has passed through one layer and furthest down through two layers of Plexiglas.

arrived first because it passed over the Plexiglas in Figs. 17 and 18. Further down we see the light that passed through one layer and furthest down the light that passed through the double layer of Plexiglas. Thus in this view we clearly see the pulse fronts as seen from the side ($\phi = 90°$) in spite of the fact that they are photographed from the same hologram as is Fig. 19, which shows the wavefront coming straight toward us ($\phi = 0$).

The manipulations of the single holographic image resulting in the transformations seen in Figs. 18–24 are similar to those manipulations of interferograms that can be made in a Michelson interferometer when one mirror is tilted at different angles. Figures 20–22 were photographed with the camera ~3 cm behind the hologram plate resulting in angle $\phi = 0$ in Fig. 16. In Fig. 23 that distance was 1.3 m, and in Fig. 24 it was 1.7 m (behind the real image).

VI. Position of the Light-Shutter

One more method exists to retrieve information from a light-in-flight hologram: reconstruct the real image of the object onto a screen of paper by illuminating the hologram plate with the conjugate of the reference beam. Make a pinhole through the paper at the image of the point on the object, the distance to which is to be measured, and look through the hole toward the hologram plate. A bright line is seen on the plate representing that part of the plate that reconstructs the studied point. What is seen is simply the reference pulse (the light shutter)[7] at the moment when the

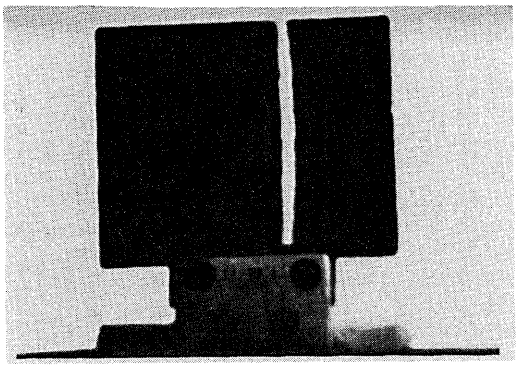

Fig. 25. Looking through one point of the real image toward the hologram plate we see a bright line across the plate. This bright line represents the position of the reference pulse (the light shutter) at the moment when that object point was recorded. Thus the horizontal position of this line is a measure of the distance to the studied object point.

studied object point was recorded. Thus the hologram plate could be equipped with a ruler indicating the time of flight or even the distance to the object.

As an example we look at Fig. 25 which is a photo of the hologram plate used to make Figs. 20–24. The plate was photographed through the bright part of the real image representing light delayed by one single layer of Plexiglas (see Fig. 21). Thus the horizontal position of the bright vertical fringe in Fig. 24 represents the time of flight which can be transformed into distance in the case of contouring as described in Figs. 8–15. In that case the reference arrived from the left (Fig. 9). However, the real image is studied from the opposite side compared with the virtual image and therefore the distances in Fig. 25 were measured from right to left. The distance to the object is calculated in the following way (see Ref. 7):

$$d = K + \frac{L \sin(\phi + \beta)}{\cos\beta}, \tag{26}$$

where d = distance to the studied object point,
K = constant time delay caused by the setup,
L = distance of bright fringe from right border of hologram plate.
ϕ = angle of the reference pulse from normal to the plate, and
β = tilt of the pulse front.

Usually the pulse front of the reference beam is not tilted and therefore $\beta = 0$. In that case Eq. (26) is simplified:

$$d = K + L \sin\phi. \tag{27}$$

VII. Reemission of Pulses

It should be pointed out that LIF not only produces images of light pulses, it can also reconstruct and reemit the pulse itself with a result slightly similar to that described in Refs. 8 and 9. If the hologram in, e.g., Fig. 9 is reconstructed by the conjugate of the reference pulse, the conjugate of the pulses that exposed the plate are diffracted out of the hologram plate. If the holographic setup is unchanged, these pulses travel to the propeller and, after being scattered by its surface at different depths, they combine and become the conjugate to the single pulse that originally illuminated the propeller.

The length of this pulse arriving back to the laser can be used as a measure of the dimensional difference between the propeller under study and the propeller that was earlier recorded in the hologram. This would be true if the same object is studied in different conditions or even if two different objects of similar shape are compared.

LIF might have the advantage over the methods described in Refs. 8 and 9 because it records the time sequence along the surface of a large hologram plate instead of through the depth of a sensitive material. This fact facilitates a larger time capacity and also makes possible remarkable manipulations of the pulse shapes.

Thus, when the holographic plate is reconstructed by a sufficiently short single pulse, it not only reconstructs the recorded pulses but also emits pulses that are identical to, or conjugate to, those recorded. The total recorded time interval is the time it took for the light shutter (the reference pulse) to move over the length of the plate, and the resolution is limited only by the length of the reference and reconstruction pulses. The method could be used to store the shape of pulses for later emission. The pulses could be manipulated, e.g., to emit in another wavelength or to become elongated or compressed. They could even be shortened so that they are turned inside out making the emitted pulse the true recorded pulse and not its conjugate. These manipulations can be made by applying tilted pulse fronts as described in Ref. 7. The tilted pulse fronts could be used in the reconstruction pulse, the reference pulse, or in the object pulse itself.

VIII. Conclusion

We have studied mathematically and graphically how wavefronts studied by light-in-flight recording by holography appear distorted by two factors. The first is relativistic effects caused by the limited speed of light; the second is caused by the holographic effect. It has been described how the latter can be used to compensate for distortions caused by the former.

In an ordinary interferometer, e.g., a Michelson type, the fringes can be explained as caused by an object surface intersected by interference surfaces that can be moved back and forth and also be tilted by changing the position and angle of one mirror. Similar results can be achieved with the light-in-flight hologram. The bright line can be explained as caused by an object surface intersected by a light sheet that can be moved back and forth and also be tilted by moving the point of observation parallel or perpendicular to the hologram plate. It is quite impressive that one single optical element, the hologram plate, permits such a variety of image manipulations during reconstruction.

Using a conjugate reference beam results in three advantages: a larger apparent tilt of the pulse front, a reading of the measured distance directly on the holo-

gram plate, and finally a reemission of the recorded pulse.

References

1. Y. N. Denisyuk, D. I. Staselko, and R. R. Herke, "On the Effect of the Time and Spatial Coherence of Radiation Source on the Image Produced by a Hologram," in *Proceedings, Applications of Holography*, Besancon (July 1970).
2. D. I. Staselko, Y. N. Denisyuk, and A. G. Smirnow, "Holographic Recording of the Time-Coherence Pattern of a Wave Train from a Pulsed Laser Source," Opt. Spectrosc. **26**, 41 (1969).
3. N. Abramson, "Light-in-Flight Recording: High-Speed Holographic Motion Pictures of Ultrafast Phenomena," Appl. Opt. **22**, 215–232 (1983).
4. N. Abramson, *The Making and Evaluation of Holograms* (Academic, London, 1981), pp. 28, 110, 144, 197.
5. N. Abramson, "Light-in-Flight Recording. 2: Compensation for the Limited Speed of the Light Used for Observation," Appl. Opt. **23**, 1481–1492 (1984).
6. N. Abramson, "Single Pulse Light-in-Flight Recording by Holography," Appl. Opt. **28**, 1834–1841 (1989).
7. N. Abramson, S. Pettersson, and H. Bergstrom, "Light-in-Flight Recording. 5: Theory of Slowing Down the Faster-than-Light Motion of the Light Shutter," Appl. Opt. **28**, 759–765 (1989).
8. R. K. Kaarli, A. K. Rebane, and P. M. Saari, "4-D Holography and Storage of Ultrafast Time-Domain Signals," in *Proceedings, International Conference on Optical Science and Engineering*, Paris (Apr. 1989).
9. C. Joubert, M. L. Roblin, R. Grousson, and P. Lavallard, "Holographic Method to Realize a Temporal Phase Conjugation Mirror by Inversion of the Spectral Phase of a Picosecond Pulse," in *Proceedings, International Conference on Optical Science and Engineering*, Paris (Apr. 1989).